Nanoscale Advances

MINIREVIEW

View Article Online
View Journal | View Issue

Cite this: *Nanoscale Adv.*, 2019, **1**, 4644

Metal oxide-based supercapacitors: progress and prospectives

Cuihua An,†[ab] Yan Zhang,†[a] Huinan Guo†[a] and Yijing Wang *[a]

Distinguished by particular physical and chemical properties, metal oxide materials have been a focus of research and exploitation for applications in energy storage devices. Used as supercapacitor electrode materials, metal oxides have certified attractive performances for fabricating various supercapacitor devices in a broad voltage window. In comparison with single metal oxides, bimetallic oxide materials are highly desired for overcoming the constraint of the poor electric conductivity of single metal oxide materials, achieving a high capacitance and raising the energy density at this capacitor-level power. Herein, we investigate the principal elements affecting the properties of bimetallic oxide electrodes to reveal the relevant energy storage mechanisms. Thus, the influences of the chemical constitution, structural features, electroconductivity, oxygen vacancies and various electrolytes in the electrochemical behavior are discussed. Moreover, the progress, development and improvement of multifarious devices are emphasized systematically, covering from an asymmetric to hybrid configuration, and from aqueous to non-aqueous systems. Ultimately, some obstinate and unsettled issues are summarized as well as a prospective direction has been given on the future of metal oxide-based supercapacitors.

Received 30th August 2019
Accepted 1st October 2019

DOI: 10.1039/c9na00543a

rsc.li/nanoscale-advances

1. Introduction

Transitional metal oxide materials have been deemed as promising candidates to be used as electrodes of energy storage devices on account of their abundant reserves, environmental geniality, easy approachability and other intriguing characteristics; for instance, their diverse constituents and morphologies, large surface area and high theoretical specific capacitance.[1–3] In addition, they play a central part in the electrodes of electrochemical supercapacitors, and offer a conspicuous capacitance improvement by adjusting and controlling their defects and surface/interfaces under a certain nanoscale.[4,5] Though their energy density has shown an enhancement to a certain degree, their low electrical conductivity, uncontrollable volume expansion and sluggish ions diffusion in the bulk phase have hindered their practical applications.[6–9] Hence, it is of utmost importance and urgency to explore functional metal oxide materials with improved electrochemical properties.

The design of metal oxide materials in terms of their composition, the fabrication of novel nanostructures, their electroconductivity and oxygen vacancies have boosted the physical and chemical performances of metal oxides, regarding their electrical conductivity, specific surface area, electro-active sites and chemical stability. First of all, the co-existence of two different cations in a single crystal structure could produce more electrons than single metal oxides, which leads to the improvement in the electrical conductivity. For instance, spinel $NiCo_2O_4$ materials possess electrical conductivity two or three orders of magnitude higher than the corresponding single metal oxide NiO or Co_3O_4 materials.[10] Also, the doping of a Ni element enhances the electrical conductivity from 3.1×10^{-5} (Co_3O_4) to 0.1–0.3 S cm^{-1} ($Ni_xCo_{3-x}O_4$).[11] Moreover, another metal doping affords original single metal oxide materials with extra redox reactions and reduces the charge transfer impedance for electrochemical supercapacitors, in which the specific capacitance is significantly larger than that of original single metal oxide materials without the cost of fast charging–discharging kinetics. Second, in comparison with bulk metal oxide materials, novel nanostructured metal oxides are usually porous and can provide a higher surface specific area, which is conducive to the infiltration of the electrodes, full contact between the active materials and electrolyte, the transportation of ions in the electrolytes and the utilization of the active materials at high rate charging–discharging.[12–15] In addition, the satisfactory electro-active sites, and chemical and high-thermal stabilities of the metal oxide materials guarantee high pseudo-capacitive performances and cyclic stability. Third, increasing number of metal oxide/C composites have been reported, including carbon nanotubes, carbon nanofibers, graphene and amorphous carbon materials, which have dramatically improved electroconductivity and further

[a]Key Laboratory of Advanced Energy Materials Chemistry (Ministry of Education), Renewable Energy Conversion and Storage Center, College of Chemistry, Nankai University, Tianjin 300071, P. R. China. E-mail: wangyj@nankai.edu.cn

[b]Tianjin Key Laboratory of Advanced Functional Porous Materials, School of Materials Science and Engineering, Tianjin University of Technology, Institute for New Energy Material & Low-Carbon Technologies, Tianjin 300384, P. R. China

† These authors contributed equally.

enhanced specific capacitance and rate performances.[16–19] Fourth, the introduction of oxygen vacancies into metal oxides leads to a larger interlayer spacing, which promotes faster charge storage kinetics with an intercalation pseudocapacitive behaviour. For example, the intercalation pseudocapacitive charge storage for MoO_{3-x} is two times larger than that for MoO_3.[20]

On account of the above unique features, the use of metal oxides has led to breakthroughs for pseudo-supercapacitors and has gradually ameliorated the energy density at the battery level without sacrificing traditional capacitor power delivery, which bridges the gap between batteries and capacitors. Compared with bulk metal oxide materials with inferior specific surface area and capacitive performances, the growing trend to design and fabricate novel porous nanostructures and composites with carbon materials is desirable to increase the surface specific area and to achieve excellent electrochemical properties.

Subsequently, the development of various devices, such as asymmetric supercapacitors (aqueous or non-aqueous systems), hybrid supercapacitors, including Li-ion hybrid supercapacitors, Na-ion hybrid supercapacitors and other novel hybrid supercapacitors and solid-state asymmetric supercapacitors have been reported, particularly the vital parameters influencing the energy density of the devices. Therefore, it has been seen that the assembled asymmetric supercapacitors with porous bimetallic oxide/C materials can deliver a competitive energy density of about 80 W h kg^{-1}, approaching that of commercial lithium-ion batteries (at the same power).[21] Besides, assembling asymmetric supercapacitors in non-aqueous solutions could offer a wider working voltage window of about 3 V, further pushing the energy density to the 100 W h kg^{-1} level. Also, the combination of high energy and power has been successfully realized in hybrid asymmetric supercapacitor systems, particularly Li-ion or Na-ion hybrid systems.[22–24]

Hence, in this tutorial review, we present the recent developments in metal oxide-based supercapacitors in detail, highlighting their importance in high energy-density integrated supercapacitors. The basic principles of the metal oxide materials and the innovative progress in multifarious supercapacitor devices have been covered intensively. Re-reading the recent literature could probably help in the understanding of this area, and reveal the future prospects for the development of supercapacitors.

2. Principal elements limiting the performance of metal oxide-based electrodes

As pseudo-capacitor type electrode materials, the theoretical specific capacitance of metal oxides can be determined by the following eqn (1):

$$C_t^s = \frac{n \times F}{M \times V} \quad (1)$$

where n is the number of electrons transferred in the redox reaction, F is the Faraday's constant, M is the molar mass of the metal oxides and V is the operating voltage window. Fundamentally, those metal oxides with a lower molar mass and more electrons to transfer potentially usually have a higher specific capacitance. Thus, different chemical constitutions, especially the valence state of the metal in single metal oxides and the components in metal oxide composites play key roles in the electrochemical performance. In addition, the specific surface area (SSA) also matters because the pseudo-capacitance process occurs at the surface of electrodes. Therefore, a much more effective SSA would offer more electro-active sites for the pseudo-capacitance process. In general, the SSA of metal oxides depends largely on their microstructures. The rational design of a microstructure with a unique pore size and suitable SSA would assist in enhancing the capacitance of metal oxide electrodes. Another issue for metal oxide electrodes is their electroconductivity. Most metal oxides usually own relatively large band gaps compared with metals and show a semiconductor behaviour. Applied as electrode materials, the poor electroconductivity still restricts their capacitance.

Besides capacitance, the energy density and power density of metal oxide electrodes are two crucial issues in practical applications. These could be obtained using the following eqn (2) and (3):

$$E = \frac{CV^2}{2} \quad (2)$$

$$P = \frac{V^2}{4R} \quad (3)$$

where C is the capacitance in farad, V is the nominal voltage and R is the equivalent series resistance (ESR) in Ohm. Obviously, the nominal voltage V (electrochemical window) plays a vital role in the energy and power density and is largely related to the electrolyte systems in supercapacitors.

According to the above discussion, we summarize that the principal elements limiting the performance of metal oxide-based electrodes is attributed to their chemical constitution, microstructure, electroconductivity and electrolytes. Subsequently, we combine recent cutting-edge research articles to elaborate the above elements and give some proposals for the further development of metal oxide-based electrodes.

2.1 Diverse chemical composition

At present, increasing number of research are focusing on the diverse chemical composition of metal oxides because single component metal oxide seem not to be able to fully meet the comprehensive performances needed for supercapacitor electrodes.[25–29] For example, He *et al.* fabricated an $FeCo_2O_4$@NiCo-LDH composite electrode displaying a remarkable specific capacitance of 2426 F g^{-1} at 1 A g^{-1}, and an ultrahigh rate capability with 72.5% capacitance retention at 20 A g^{-1}. Such excellent performances could be attributed to the combination of these two species and abundant electrochemical active sites on this composite.[25] Moreover, Zhang *et al.* fabricated a self-assembled $NiCo_2O_4/MnO_2$ composite electrode displaying a large areal capacitance of 13.9 F cm^{-1} at 4 mA cm^{-1} and the aqueous asymmetric device built by this electrode delivered

a high energy density (60.4 W h kg^{-1}) and power density (950.1 W kg^{-1}).[26] On the one hand, the diversity of metal oxides would be enriched by the variety and valence of metal ions, which present higher electrochemical activity. On the other hand, the synergistic effect between different species would enhance the overall performances of diverse metal oxides by facilitating such activities as ion adsorption, diffusion and transport compared with single metal oxides.

Apart from the diversity of metal oxides, the construction of metal oxides and other materials, such as hydroxides, metal quantum dots and organics, has also emerged over the past few years.[22–24] The chemical composition of metal oxide-based electrodes varies diversely, but fully understanding the detailed synergistic effect from different components to rationally design the electrodes still deserves further study.

2.2 Microstructure and electroconductivity

It has been widely accepted that nanomaterials possess unique physical/chemical properties, particularly in the interfaces compared with general bulk materials. Similarly, the microstructures of metal oxide-based electrodes also deeply influence their electrochemical performances. Some essential parameters, such as specific surface area, solid diffusion of ions and wettability with electrolytes depend on the microstructures of the electrodes to a great extent. Various metal oxides with all kinds of nanostructures have been rationally obtained to enhance their performances. For example, 1D $NiCo_2O_4$ nanowire-coated rGO delivered a high specific capacitance of 1248 F g^{-1} due to its unique interfacial effect with electrolytes.[30] 2D $MnMo_4{\cdot}H_2O@MnO_2$ nanosheets possessed a specific capacitance of 3560.2 F g^{-1} (at 1 A g^{-1}) with an energy density of 45.6 W h kg^{-1} at a power density of 507.3 W kg^{-1}.[31] 3D hollow $NiCo_2O_4$ nanospheres with a large specific surface area also reached a capacitance of 1229 F g^{-1} (at 1 A g^{-1}), remarkable rate performance and good cycle performances (as shown in Fig. 1a–c).[32] Different nanostructures with different dimensions possess their own unique advantages and an accurate control for obtaining special nanostructures is a challenging task.

Recently, metal oxides, with controllable microstructures derived from metal–organic frameworks (MOFs), have gradually become the mainstream in the supercapacitor field (Fig. 2a–c).[33,34] For instance, Lou *et al.* reported seven-layered Ni–Co oxide spheres derived from MOFs (Fig. 1d–i) with a capacitance as high as 1900 F g^{-1}, good rate capability and ultrahigh cycling stability (93.6% retention over 20 000 cycles), which should be attributed to the microstructural advantage that the volume change in the oxide nanograins was well-accommodated at the shell level.[34] Several special reviews on metal oxides derived from MOFs are provided for readers to further understand as detailed syntheses and other topics are beyond this paper.[35,36] The control of metal oxides with desired microstructures can be realized by the introduction MOFs as precursors, and relevant metal oxides derived from them show quite competitive performances, but research in this field seems to be in a jam as the present MOF precursors only focus on several typical MOFs. Thus, the exploration of novel MOFs as new precursors to synthesize metal oxides with unique microstructures is urgently needed, particularly considering that inorganic chemists have synthesized numerous MOFs waiting to be tested for applications.

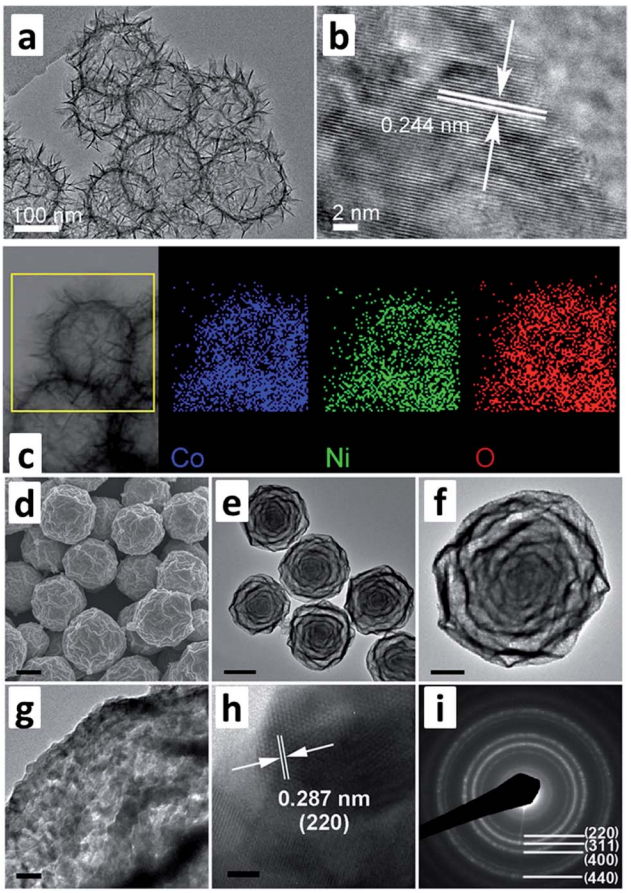

Fig. 1 (a–c) TEM images and EDS mapping of three dimensional $NiCo_2O_4$ nanospheres, (d–i) SEM and TEM images of seven-layered Ni–Co oxide spheres derived from MOF (modified from ref. 32 and 33, copyright permission from Elsevier and Wiley-VCH, respectively).

Another usually criticized issue of metal oxide-based electrodes is their electroconductivity. Indeed, the intrinsic electroconductivity of metal oxides depends on their band gap and is usually unsatisfactory compared with other supercapacitor electrodes, such as carbonaceous electrodes.[37] Fortunately, the use of compositing, element doping and the intentional creation of oxygen vacancies (V_O) could be conducted to improve the electroconductivity of metal oxide-based electrodes.

Among the above three strategies, the compositing of metal oxide electrodes with other high electroconductivity materials is a popular way. Recently, a large family of 2D transition metal carbides and nitrides, collectively referred to as MXenes, have attracted considerable attention due to their metallic electrical conductivity, which make them a novel electroconductivity carrier to be composited with metal oxides. For example, self-assembled MXene (Ti_3C_2TX)/alpha-Fe_2O_3 nanocomposite electrodes showed capacities of 405.4 F g^{-1} (2 A g^{-1}), 289 F g^{-1} (10 mV s^{-1}) and 97.7% capacity retention after 2000 cycles

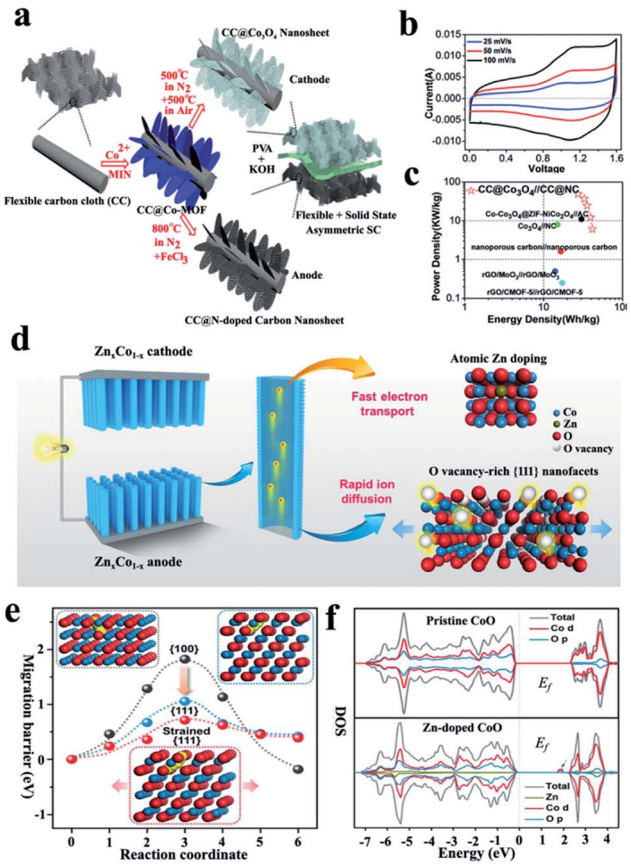

Fig. 2 (a) Schematic of the "one for two" fabrication process: a 2D Co_3O_4 nanosheet cathode and N-doped carbon nanosheet anode are obtained from the same Co-MOF precursor, (b) CV curves and (c) Ragone plot of a CC@Co_3O_4//CC@NC asymmetric supercapacitor with a PVA–KOH gel electrolyte (modified from ref. 34, copyright permission from the Royal Society of Chemistry); (d) schematic of the atomic-level structure engineering of $Zn_xCo_{1-x}O$ for high-rate intercalation pseudocapacitance applications and (e and f) computational investigations of oxygen-ion diffusion and electrical conduction in $Zn_xCo_{1-x}O$ (modified from ref. 47, copyright permission from the American Association for the Advancement of Science).

(100 mV s^{-1}).[38] Besides MXenes, compositing metal oxides with other high electroconductivity materials, such as carbonaceous materials (including carbon nanotubes, graphene and other carbon materials) and electroconductive polymers are still carried out by many researchers.[39–41] Regarding the compositing of metal oxides with carbonaceous materials, some related studies have been carried out. Carbonaceous materials synthesized from biomass hold great promise due to their wide resources and as they fit in with the idea of the recycle economy. For example, a hierarchal structure of Co_3O_4@biomass-derived carbon fiber@Co_3O_4 was fabricated and a high capacitance of 892 F g^{-1} was observed in this sandwich composite.[42] As a beneficial reference, Chen *et al.* investigated the supercapacitor behaviour of a graphene–polypyrrole hybrid, which provides a guideline for further research.[43] Recently, graphdiyne has emerged as a novel carbon material with a high degree of π conjugation. Its unique electronic structure and uniformly distributed pores have made it possible to store lithium and sodium, so some studies on the compositing of metal oxides and graphdiyne perhaps deserve further research.[44,45] Regarding the compositing of metal oxides with electroconductive polymers, some feasible examples could also be found. Li *et al.* synthesized $FeCo_2O_4$@polypyrrole core/shell nanowires, which displayed a specific capacitance of 2269 F g^{-1} as well as showing excellent cycle performance.[46] The interfacial engineering between metal oxides and organic electroconductive polymers is a key issue and the development of a simple method to synthesize organic electroconductive polymers and to composite such with metal oxides effectively is also challenging.

Different from compositing metal oxides with high electroconductivity materials, element doping and the intentional creation of oxygen vacancies can also improve the intrinsic electroconductivity of metal oxides by modulating their band gap. Qiao *et al.* reported the radical modification of $Zn_xCo_{1-x}O$ *via* atomic-level structure engineering and the obtained $Zn_xCo_{1-x}O$ exhibited a high rate performance with a capacitance up to 450 F g^{-1} at a scan rate of 1 V s^{-1} due to its fast ion and electron transports, pushing its capacity almost to the theoretical limits.[47] Fig. 2d–f display the atomic-level structure engineering of $Zn_xCo_{1-x}O$ and computational investigations of oxygen ion diffusion and electrical conduction in the $Zn_xCo_{1-x}O$. Another recent example could be found in Mn-doped Co_3O_4 mesoporous nanoneedle arrays, which delivered a high capacitance of 668.4 F g^{-1} compared to that of undoped Co_3O_4 201.3 F g^{-1} at 1 A g^{-1} and excellent capacitance retention (104% after 10 000 cycles at 6 A g^{-1}).[48]

More recently, the intentional creation of oxygen vacancies (V_O) has been explored to improve the intrinsic conductivity and electrochemical activity of transition metal oxides, and thus to increase their supercapacitor performance. As a pioneering study, Dunn *et al.* studied the enhanced pseudocapacitive charge storage property of MoO_{3-x} with oxygen vacancies.[20] After that, Yang *et al.* reported oxygen-vacancy abundant ultrafine Co_3O_4/graphene composites for high-rate supercapacitor electrodes with a high capacitance of 978.1 F g^{-1} (1 A g^{-1}).[49] Such a strategy also seems to be an effective way to improve the intrinsic conductivity of metal oxides and deserves extending to other metal oxides.[50]

According to the above discussions, we could conclude that their diverse chemical constitution provides a guideline to find potential novel metal oxides with considerable performance for supercapacitors. Moreover, the diversity of metal oxides with other functional species could cover the shortage of single metal oxides. However, for a given metal oxide, its microstructure and electroconductivity affect its performance deeply. Thus, the rational design of metal oxides with special microstructures and the enhancement of their electroconductivity would help them obtain better performances.

2.3 Various electrolytes

Electrolytes also have vital functions in the supercapacitor performance. In general, the decomposition potential range of electrolytes controls the breakdown voltage of supercapacitors,

which limits their energy and power densities. A high operating voltage could provide both a high energy density and power density. Moreover, the ionic conductivity of electrolytes is another important parameter related to power density. Other requirements to take into account in electrolytes include the temperature coefficient, high electrochemical stability, high ionic concentration, low solvated ionic radius, low viscosity, low volatility, low toxicity and low cost. At present, the main electrolytes used in supercapacitors could be summarized as aqueous electrolytes, organic electrolytes and ionic liquid electrolytes. Every electrolyte has its own advantages and disadvantages, which are introduced in the following.

2.3.1 Aqueous and organic electrolytes. The aqueous electrolytes currently employed can be divided into three types: acidic solutions (such as H_2SO_4 solution), alkaline solutions (such as KOH solution) and neutral solutions (such as Li_2SO_4 and Na_2SO_4 solutions). Aqueous electrolytes provide a relatively higher ionic concentration and lower resistance, which are beneficial for higher capacitance and rate performances.[51] However, limited by the thermodynamic decomposition of water, aqueous electrolytes own a narrow electrochemical window, restricting the energy density of aqueous electrolyte-based supercapacitors. Of course, aqueous electrolytes could be employed in some situations, where cost is more important instead of energy density. In contrast, organic electrolytes provide a much wider electrochemical window, which allows for a higher energy and power density. Obviously, organic electrolytes are more expensive due to their purification from water. In addition, as commonly used solvents in organic electrolytes, acetonitrile (ACN) and propylene carbonate (PC) are usually blamed for their flammability, which results in a potential safety issue in practice. So, different electrolytes possess relative merits and should be rationally chosen in various practical situations, where a certain parameter is more important.

Recently, the concept of "water-in-salt" to broaden the electrochemical window of aqueous electrolytes and to settle the flammability issue of organic electrolytes has been attracting considerable attention. In 2015, Wang *et al.* reported an ultrahigh concentration of a LiTFSI "water-in-salt" (WIS) electrolyte, which provided a wide stable electrochemical window and displayed an extended cathodic and anodic potential of 1.9 V and 4.9 V *vs.* Li^+/Li, respectively.[52] Inspired by that, Zhang *et al.* constructed a hybrid supercapacitor consisting of metal oxide electrodes in a "water-in-salt" electrolyte. As shown in Fig. 3a–c, the hybrid Fe_3O_4/21 M LiTFSI/MnO_2 capacitor displayed an operating voltage of 2.2 V and a high specific energy of 35.5 W h kg_{total}^{-1}.[53] Moreover, Yu *et al.* summarized some key tips on supercapacitors based on "water-in-salt" electrolytes.[54]

Although the working potential window of the reported WIS systems has improved dramatically, environmental and economic concerns related to their practical applications still need to be solved. In particular, the high cost of LiTFSI salt hinders its large-scale feasibility, while the other hydrate melt components (LiBETI) only represent a small quantity with high cost (>40 \$ g^{-1}).[55] Another important issue is the lower crustal reserves of metal Li, compared with the main group of metal Na and K. Therefore, in order to configure WIS electrolytes, a huge

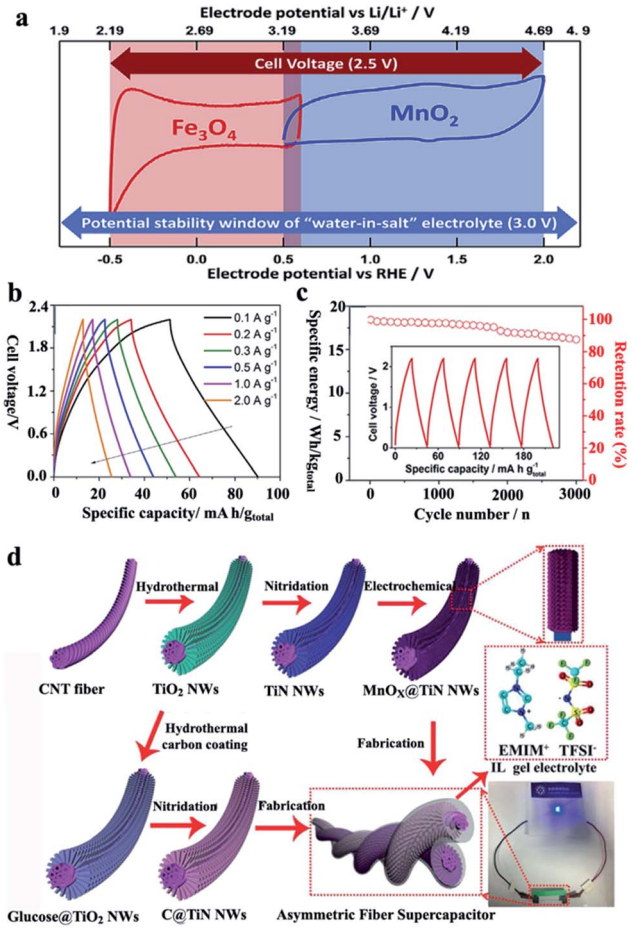

Fig. 3 (a) CV curves of Fe_3O_4 and MnO_2 electrodes in a 21 M LiTFSI electrolyte, (b) galvanostatic charge/discharge curves and (c) specific energy retention of an asymmetric supercapacitor of Fe_3O_4/21 M LiTFSI/MnO_2 (modified from ref. 53, copyright permission from Elsevier); (d) schematic of the fabrication processes for a MnO_x@TiN nanowire@carbon nanotube fiber and C@TiN electrode-based asymmetric fiber supercapacitor with an ionic liquid gel electrolyte (modified from ref. 59, copyright permission from the Wiley-VCH).

amount of LiTFSI salts must be further considered. As for environmental issues, the dermal toxicity and acute oral of LiTFSI salts may be considered toxic to the environment. Therefore, Bao *et al.*[56] fabricated potassium acetate-based WIS electrolytes, which could offer the same broad working potential voltage as LiTFSI-based WIS electrolytes, while also being low priced and environmental friendly.

Moreover, the rate capability of these aqueous batteries fabricated with super-concentrated WIS electrolytes are restricted by their ultrahigh viscosity and ultralow conductivity due to their strong electrostatic attractions.[52,54] Moreover, WIS electrolytes are usually highly concentrated or nearly saturated, which make them easily precipitated out.[52,57] The above fact further hinders the wide-temperature-range applications of WIS electrolytes for batteries. However, it is a great challenge to solve the problems of high viscosity, low conductivity and precipitation without sacrificing the broad working potential window and the fire-distinguishing capability of the WIS electrolyte.

Hence, Yan *et al.* introduced acetonitrile into a conventional WIS electrolyte to form an "acetonitrile/water-in-salt" (AWIS) system.[58] The 5 M AWIS electrolyte provided decreased viscosity, enhanced conductivity and a wide liquid temperature range while also retaining the vital superiority of the WIS system, such as its safety, broad working potential window and moisture resistance.

2.3.2 Ionic liquid electrolytes. Ionic liquids (ILs), also called room-temperature molten salts, are composed entirely of ions and are solvent-free and liquids at room temperature. They are regarded as the third kind of electrolytes, following aqueous and organic electrolytes. Moreover, ILs are typically characterized by high thermal and chemical stabilities, low flammability, low toxicity and particularly an extended electrochemical window up to 6 V. For instance, a fiber metal oxide-based asymmetric fiber supercapacitor with an ionic liquid gel electrolyte (Fig. 3d) shows a wide voltage window, allowing for a higher volumetric energy density and power density.[59] Although ionic liquid electrolytes show promising potential, their highly viscous property results in a low ionic conductivity. In addition, the interface between electrodes and the ionic liquid is different from that of traditional aqueous and organic electrolytes and seems more challenging, and thus deserves more investigation.

3. Supercapacitor devices

In general, supercapacitor devices (SCDs) are energy storage configurations that can achieve a high power density, rapid charge/discharge and extremely long-term cyclic stability.[22,60] Hence, SCDs have attracted the ever-increasing interest of researchers for energy storage and conversions. In the following sections, a variety of SCD-based on metal oxide electrodes are discussed.

3.1 Aqueous asymmetric supercapacitor devices based on metal oxides

In general, aqueous asymmetric supercapacitor devices (AASCDs) are assembled by two different electrode materials (cathode and anode) with one electrode taking part in a faradaic reaction and the other one taking part in electric double-layer absorption/desorption. AASCDs possess the metrics of high specific capacitance, low-cost and excellent ionic conductivity.[61,62] Nevertheless, the energy densities for AASCDs are unsatisfactory to achieve practical applications. The key to overcoming the challenge is to explore and design suitable electrode materials. Metal oxides can be used both as anode and cathode materials of AASCDs to provide higher energy densities. In the past few years, metal oxides, mainly including single metal oxides (such as Fe_2O_3, V_2O_5, RuO_2, MnO_2, MoO_3 and WO_3), bimetallic oxides (conversion-type MN_2O_4, where M or N = Ni, Co, Zn, Mn, Fe, Cu, *etc.* and intercalation-type ($LiCoO_2$, $LiMn_2O_4$, *etc.*)) and metal oxide heterostructures, have been widely investigated as electrode materials for AASCDs. For single metal oxides, Fe-based, V-based, Ru-based, Mn-based, Co-based and other electrode materials are introduced as follows.

3.1.1 Fe based. Iron oxides, particularly Fe_2O_3 and Fe_3O_4, have attracted widespread attention from researchers as potential anode materials for AASCDs, owing to their high specific capacitance, low-cost and environmental friendliness. However, their large volume expansion and limited electric conductivity impede their further practical applications. Constructing nanostructures and incorporating them with a highly conductive matrix are valid ways to overcome the above challenges. Yan *et al.* designed an electrode material of Fe_3O_4 nanospheres decorated on graphene nanosheets *via* a facile solvothermal procedure.[63] When assembled as an anode for a supercapacitor, the fabricated graphene/Fe_3O_4//graphene/MnO_2 AASCD displayed an excellent energy density of 87.6 W h kg^{-1} and superior cycling stability of 93.1% capacity retention after 10 000 cycles. In addition, Li *et al.* demonstrated that a trimmed aligned Fe_2O_3 nanoneedle array (Fe_2O_3 NNAs) anode of AASCD presented outstanding performances. The specific energy density was as high as 103 W h kg^{-1} at the power density of 3.5 kW kg^{-1}, and the capacitance retention in long-term cycling was 86.6% after 5000 cycles.[64]

3.1.2 V based. Vanadium-based oxides have the merits of high power density, natural abundance and high theoretical specific capacity. Nevertheless, unsatisfactory structural stability and poor electric conductivity block their application fields. Vanadium oxides mainly include VO_2, V_2O_3 and V_2O_5, where the valence of +5 is the most stable and +4 is the worst. As an electrode material, V_2O_5 has been widely investigated as an AASCD cathode; however, the research on VO_2 as anode materials need to be further deepened. Anchoring with carbon-based materials is employed to overcome the obstacle of poor conductivity. Recently, Lee *et al.* demonstrated that a mixed VO_2 matrix with V^{4+} state and a significant amount of V^{3+} state could behave as a negative electrode with a working potential of −1 to 0 V *vs.* Ag/AgCl.[65] When used as an anode of AASCD, the Mn_3O_4 cathode exhibited a high energy density of 42.7 W h kg^{-1} and a power density of 1.1 kW kg^{-1}.

3.1.3 Ru based. Considering its high theoretical specific capacitance (1700 F g^{-1}), good electric conductivity (105 S cm^{-1}) and reversible redox reaction, RuO_2 is recognized as one of the most promising AASCD electrodes. In addition, RuO_2 has good corrosion resistance to acidic and basic environments, promising wide applications for aqueous systems with different aqueous electrolytes. Amorphous hydrous $RuO_2 \cdot xH_2O$ and crystal phase RuO_2 are the two phases of ruthenium oxide. Here, the former has a higher capacitance and larger active sites. Hydrous RuO_2 was first demonstrated as a pseudocapacitive electrode material in an acidic electrolyte for a supercapacitor by Buzzanca *et al.* in 1971.[66] However, one of the biggest challenges of the RuO_2 electrode is the serious agglomeration during cycling. Cao *et al.* fabricated a unique nanostructure material, consisting of RuO_2 nanoparticles (diameter of 1.9 nm) anchored on graphene nanosheets and carbon nanotubes, which could effectively inhibit the agglomeration phenomenon.[67]

3.1.4 Mn based. Manganese oxide materials have been broadly investigated for the cathode materials of AASC devices. Among these, MnO_2 and Mn_3O_4 have attracted considerable attention for applications owing to their low cost, wide operating potential window and earth abundance nature. Efforts have been focused on crossing the gap between theoretical capacitance and experimental capacitance. Zhang *et al.* tailored a core–shell structure electrode consisting of a β-MnO_2 core and highly aligned "birnessite-type" MnO_2 shell.[68] A packaged AASCD delivered a high energy density of 40.4 W h kg^{-1} with a maximum power density of 17.6 kW kg^{-1}. Recently, several groups have demonstrated that the insertion of a high content of cations (*e.g.* Na^+ and K^+) into the MnO_2 structure can accomplish enhanced electrochemical performances, depending on the additional redox reaction.[69,70] Xia *et al.* constructed an AASCD with $Na_{0.5}MnO_2$ nanowall arrays as a cathode and carbon-coated Fe_3O_4 nanorod arrays as an anode, exhibiting an excellent energy density of 81 W h kg^{-1} in an extended potential window of −1.3 to 0 V *vs.* Ag/AgCl.[71]

3.1.5 Co based. Among a variety of metal oxides for AASCD, Co_3O_4 cathode materials are controlled by diffusion in the electrochemical process in an aqueous electrolyte and are considered battery-type electrode materials. The Co_3O_4 cathode has been vigorously developed due to its ultrahigh specific theoretical specific capacitance and impressive redox reversibility. Nevertheless, the cycling stability and rate capability are hindered by its low electric conductivity. Therefore, considerable endeavours have been concentrated on designing nanostructured Co_3O_4 materials to improve the electrochemical performances. Yu *et al.* reported Co_3O_4/N-doped carbon hollow spheres (termed as Co_3O_4/NHCSs) with a hierarchical nanostructure as an advanced electrode for a high performance asymmetric supercapacitor device.[72] When assembled as a cathode to fabricate an AASCD, the device delivered a large energy density of 34.5 W h kg^{-1} (at a power density of 753 W kg^{-1}).

3.1.6 Others. Alongside the increasing demand for energy storage, several other metal oxide materials have been studied for AASC devices, including MoO_3,[73] WO_3,[74,75] PbO_2,[76] SnO_2 (ref. 77) and CuO.[78,79] NiO is a potential anode material for supercapacitors. Wei *et al.* synthesized honeycomb-like mesoporous NiO microspheres *via* a hydrothermal reaction as a high performance cathode for AASCD.[80] Based on the honeycomb-like NiO cathode and rGO anode, the successfully fabricated asymmetric supercapacitor achieved a remarkable energy density of 23.25 W h kg^{-1} and an excellent power density of 9.3 kW kg^{-1}, which was sufficient for lighting up a light-emitting diode. Moreover, CuO has become a hopeful candidate electrode material for its elemental abundance. Kaner *et al.* built a three-dimensional ordered CuO framework with bimodal nanopores and nanosized walls (about 4 nm).[81] The assembled AASCD with an activated carbon electrode demonstrated an energy density of 19.7 W h kg^{-1} and excellent cycling life.

Compared to single metal oxides, bimetallic oxides integrate the advantages of various metal oxides to work together for AACSDs.[82–84] Recently, our research group presented a yolk–shell-structured $ZnCo_2O_4$ with uniform carbon (Fig. 4a) for an aqueous asymmetric supercapacitor, displaying a remarkable cycling stability with a capacitance retention rate of over 95% after 9000 cycles and a high energy density of 45.9 W h kg^{-1} (at a power density of 700 W kg^{-1}), as shown in Fig. 4b.[85]

In addition, it is noticeable that various pseudocapacitive metal oxide heterostructures have provoked the broad interests of researchers and are being studied.[86] Owing to the defects of contact surfaces and the synergistic effects of different phases, such heterostructures can provide more active sites and improve the electric conductivities, and so have been firmly identified as a hopeful structure to reinforce the electrochemical performances of AASCDs.[84,87] A hierarchical core–shell-like NiO–Co_3O_4–NiO nanoheterostructure was fabricated by a simple solution-based method to increase the interaction abilities of aqueous electrolyte ions diffusing into the bulk materials. When assembled as an AASCD (Fig. 4c) with NiO–Co_3O_4–NiO with fish thorn-like nanostructures (FTNs) as the positive electrode and porous activated carbon loaded on nickel foam (AC@NF) as the negative, the obtained coulombic efficiency (99.7%) at the end of cycling test further indicated the outstanding reversibility of the device (Fig. 4d).[88]

3.2 Quasi-/all-solid-state supercapacitor devices based on metal oxides

3.2.1 Generalized quasi-/all-solid-state supercapacitor devices. Taking into account the ever-growing demands and gradual developments of flexible energy storage devices, it is crucial to make adequate efforts to exploit the applications of quasi-solid and all-solid-state supercapacitor devices (QSSSCDs and ASSSCDs), which have the features of more safety, lighter weight, higher power density and more easily tailored nature.[89–91] The main progress of QSSSCDs/ASSSCDs over conventional supercapacitors is the introduction of a quasi-solid or all-solid-state electrolyte to take the place of the aqueous electrolyte, sequentially increasing the potential for applications in portable and wearable devices.

Nevertheless, the wide applications of QSSSCDs/ASSSCDs have been limited by the relative lack of electrode materials. In recent years, increasing number of metal oxide electrode materials have been applied in QSSSCs/ASSSCs to enhance the electrochemical performances. Niu *et al.*[92] fabricated a foldable ASSSCD integrated with photodetectors in a simplified paper-like configuration based on TiO_2 nanoparticles. TiO_2 nanoparticles were coated on the surface of a SWCNT film to serve as a supercapacitor electrode and working electrode of a photodetector (Fig. 5a). The assembled devices not only maintained the capacitance behaviour but also exhibited excellent sensitivity for white light. More importantly, the capacitance behaviours of ASSSCs almost remained unchanged even when the ASSSCs were folded by 180° (Fig. 5b). In addition, Wang *et al.*[93] successfully deposited MnO_2 and polypyrrole (PPy) on 3D graphene-wrapped nickel foam (Ni/GF) substrates, respectively, and tailored a flexible ASSSCD assembled with Ni/GF/PPy as the negative electrode and Ni/GF/MnO_2 as the positive electrode in a gel electrolyte. The optimized flexible ASSSCD verified

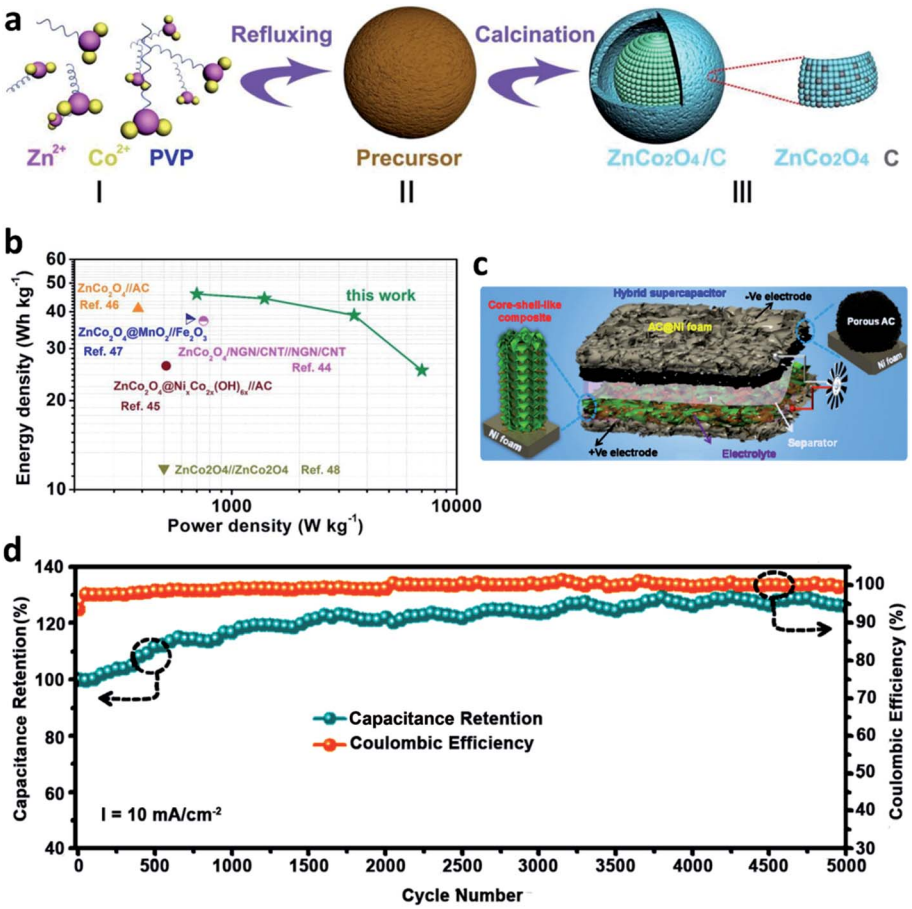

Fig. 4 (a) Scheme of the synthesis a yolk–shell structure $ZnCo_2O_4$ material, (b) Ragone plots of AACSDs (modified from ref. 85, copyright permission from the Royal Society of Chemistry); (c) illustration for the preparation process and (d) cycling stability of core–shell-like NiO@Co_3O_4–NiO FTN/Ni foam (modified from ref. 88, copyright permission from Elsevier).

a remarkable stability with 90.2% capacity remaining after 10 000 cycles in a high voltage window of 1.8 V and delivered an excellent energy density of 1.23 mW h cm^{-3}. Hence, the rational design of ASSSCs will pave the way for combining energy storage devices and other electronic equipment into one flexible device.

In addition, the contact between the solid electrolyte and electrode materials is a determining factor for enhancing the electrochemical characteristics of supercapacitors. Quasi-solid-state electrolytes offer the advantages of an all-solid-state electrolyte and liquid electrolyte, accelerating the kinetics process of ion transfer in QSSSCDs. Jun *et al.*[50] suggested a new fluorine-doped oxygen-deficient Co_2MnO_4 (denoted as F-Co_2MnO_{4-x}) nanowires coated on carbon fibers as an advanced electrode material (Fig. 5c) for QSSSCDs. The experimental and theoretical studies revealed that the structural and electronic properties of F-Co_2MnO_{4-x} were effectively adjusted by introducing fluorine element and O vacancies, which could synergistically provide newly generated energy levers and improve the reactivity of the electrochemically active sites, while at the same time providing for abundant Faradaic redox activity. A quasi-solid-state asymmetric supercapacitor device was assembled with a positive electrode of F-Co_2MnO_{4-x}/CF and a negative electrode of Fe_2O_3/CF, and achieved a high energy density of 64.4 W h kg^{-1} (at a power density of 800 W kg^{-1}), as shown in Fig. 5d. Significantly, a capacitance retention of 89.9% was maintained after 2000 bending tests with a bending angle ranging from 0° to 30°, demonstrating the excellent mechanical flexibility.

3.2.2 Flexible/stretchable supercapacitor devices. The popularization of wearable devices has stimulated the improvement of flexible/stretchable supercapacitors (FSSCDs/SSSCDs) to benefit from their remarkable features of high security, small volume, wide operating temperature range and easy integration property.[94–96] However, when integrated into flexible devices, FSSCDs/SSSCDs using liquid electrolytes are prone to suffering from the issue of electrolyte leakage.[97] Therefore, FSSCDs/SSSCDs are mainly configured with all-solid-state or gel-state electrolytes. Although flexible/stretchable supercapacitors with good flexibility are widely investigated, significant challenges remain in terms of improving their energy density without influencing their power density, and here, developing high-energy electrode materials is an effective route to overcome these difficulties.

Kim *et al.*[98] designed a novel bi-stacked WO_3 nanotube/PEDOT:PSS electrode (Fig. 6a) for a wearable patch device with polyacrylamide (PAAm) hydrogel electrolytes. With the

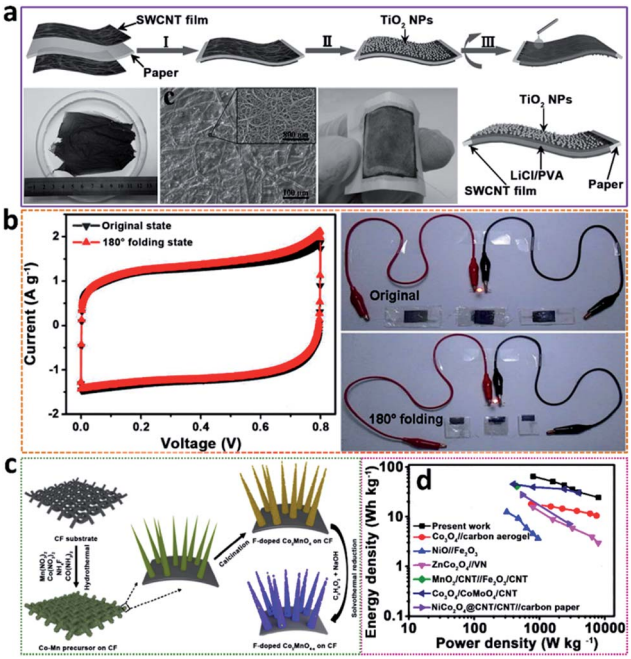

Fig. 5 (a) Schematic of the as-prepared supercapacitor–photodetector integrated device, (b) CV curves and LED lit images of three all-solid-state integrated devices with the original state and in a 180° folding state at a scan rate of 50 mV s^{-1} (modified from ref. 92, copyright permission from Wiley-VCH); (c) representative synthesis of F–Co_2MnO_{4-x} nanowires on CF substrate, (d) Ragone plots of the assembled F–Co_2MnO_{4-x}/CF//Fe_2O_3/CF QSSSCDs (modified from ref. 50, copyright permission from Elsevier).

introduction of the PEDOT:PSS wrapping layer, the coloration efficiency and specific capacity of the WO_3 nanotube electrode were improved by 20.4% to 83.9 cm^2 C^{-1} and 38.6% to 471.0 F g^{-1}, respectively. The enhanced electrochemical capacities also had a positive effect on the energy and power densities with an all-transparent stretchable electrochromic supercapacitor (all-TSES) presenting a power density of 19.1 kW kg^{-1} and energy density of 52.6 W h kg^{-1} (Fig. 6b). Moreover, as shown in Fig. 6c, the all-TSES wearable patch device showed excellent reliability, even under repeated stretching–bending motions, which confirmed its suitability for wearable applications.

In addition, Wang *et al.*[99] reported two types of composite network electrodes (Fig. 6d): MnO_2–graphene and carbon nanotube–graphene by solution casting and subsequent electrochemical methods. On the one hand, the MnO_2 nanocomposite with graphene has synergistic effects by combining the high surface area/conductivity and redox reaction of the metal oxide to improve the electrochemical properties. On the other hand, CNTs possess mechanical flexibility, good conductivity and stable electrochemical behaviour. Therefore, the assembled flexible all-solid-state asymmetric supercapacitor, based on the two composite networks, exhibited outstanding rate capability and high specific capacitances, when cycled reversibly in a high voltage region of 0 to 1.8 V (Fig. 6e).

3.3 Metal-ion hybrid supercapacitor device based on metal oxides

Although traditional supercapacitors can provide high power densities, the energy densities still do not match the growing needs of energy storage devices. A metal-ion hybrid supercapacitor device (MIHSCD) rooted in an aqueous asymmetric device is a relatively novel device, and is a combination of a battery and supercapacitor, with the aim to deliver high energy, large power and a long lifespan.[100,101] MIHSCDs belong to a kind of asymmetric supercapacitor devices. The difference is that MIHSCD consists of one battery-type faradaic electrode and one capacitive electrode, while the ASCDs refer to a wider range. At present, tremendous efforts have been focused on the architectural designs of electrode materials and the configurations of systems to achieve win–win hybrid supercapacitors. As the electrodes of MIHSCDs, metal oxides possess potential advantages of high energy, good conductivity and low-cost.

3.3.1 Li-ion hybrid supercapacitor devices. Table 1 summarizes a performance comparison of various LIHSCDs.[102–113] At present, Li-ion hybrid supercapacitor devices (LIHSCDs) are the dominant technology and have been diligently researched.[114] Nanostructural metal oxide electrode materials and their hybrids with various carbon matrixes have been investigated for LIHSCDs.[115] Among these, niobium-based oxide can be a kind of glorious electrode to realize a high performance hybrid capacitor. Chen *et al.*[116] synthesized a unique N-doped T-Nb_2O_5/tubular carbon hybrid structure (noted as N-NbOC) anode (Fig. 7a), in which T-Nb_2O_5 nanoparticles were homogeneously dispersed in N-doped microtubular carbon. The unique nano-architecture provided a porous nanostructure and enhanced electronic conductivity to favour sufficient and rapid Li-ion storage. The as-prepared LIHSCD based on the N-NbOC electrode delivered an excellent energy density of 86.6 W h kg^{-1} and a high power density of 6.09 kW kg^{-1} (Fig. 7b). In terms of other metal oxides, Li *et al.*[117] designed a non-aqueous LIHSCD with a SnO_2–C hybrid (ultrafine SnO_2 anchored on the tubular mesoporous carbon) as the anode and tubular mesoporous carbon as the cathode, achieving an energy density of 110 W h kg^{-1} at a power density of 2960 W kg^{-1}. Zhou *et al.* presented high-power LIHSCDs based on a well-designed MnO–graphene composite (MnO@GNS) and 3D hierarchical porous N-doped carbon (HNC), which achieved an attractive energy storage of 127 W h kg^{-1} electrode, which even remained as high as 83.25 W h kg^{-1} at a battery-inaccessible power density of 25 kW kg^{-1} together with rapid charging within 8 s.[112]

Bimetallic oxides have also been applied in LIHSCDs in recent years. Lei *et al.*[118] synthesized a nanocomposite with a $TiNb_2O_7$ network *in situ* anchored on holey graphene (labelled as TNO/HG, Fig. 7c), which was assembled as an anode material for LIHSCD. The as-prepared LIHSCD consisting of the nanocomposite electrode and activated carbon exhibited an excellent energy density of 86.3 W h kg^{-1} at 237.7 W kg^{-1} and a superior power density of 3.88 kW kg^{-1} at 28.7 W h kg^{-1} (Fig. 7d), accompanied with a long-term cycling stability of 90.2% capacity retention after 3000 cycles. Furthermore, the

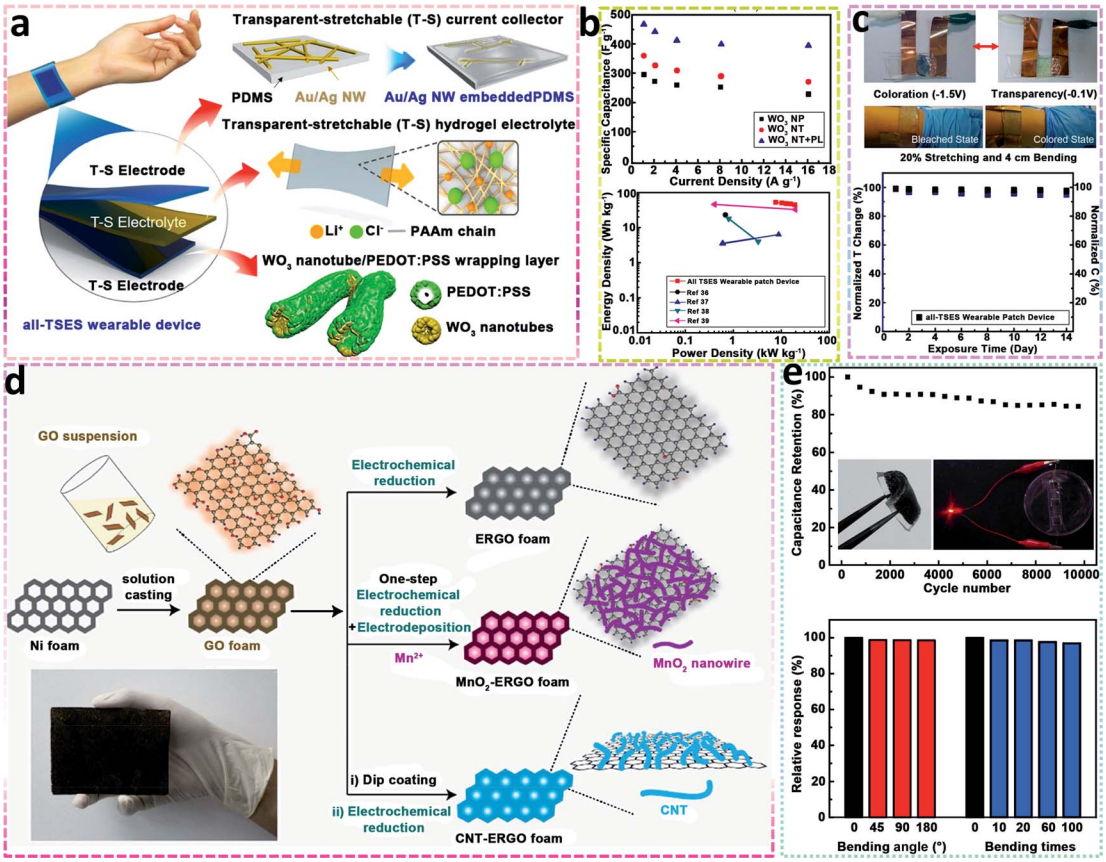

Fig. 6 (a) Schematic of an all-transparent stretchable electrochromic supercapacitor device, (b) specific capacitance and Ragone plot of all-TSES electrodes, (c) real image of bleached/coloured state and the stability property of a wearable patch device after exposure in ambient conditions for 14 days (ref. 98, copyright 2019 American Chemical Society); (d) illustration of the preparation of different nanohybrid foams, (e) cycling behaviour and specific capacitance retention ratio of a flexible all-solid-state asymmetric supercapacitor of MnO_2–ERGO//CNT–ERGO (ref. 99, copyright 2014 Wiley-VCH).

electrochemical results showed a good rate performance with a capacity retention of 73.5% (0.05–5 A g^{-1}).

3.3.2 Na-ion hybrid supercapacitor devices. Na-ion hybrid supercapacitor devices (NIHSCDs) are regarded as emerging applications that have rapidly drawn the attention of researchers with the ever-increasing price and dwindling of lithium resources. NIHSCDs possess low expenditure, a low redox potential (2.71 V) close to that of Li^+/Li (3.02 V) and an infinite sodium source, making them a potential candidate for use in larger scale supercapacitor devices.[119–121] However, one of the obstacles to developing NIHSCDs is the imbalance in the kinetics from different charge storage mechanisms between the

Table 1 Performance comparison of various LIHSCDs

Hybrid system	Energy density (W h kg^{-1})	Maximum power density (W kg^{-1})	Ref.
AC//V_2O_5/CNT	24–30	850	102
GDY//AC	95–110	1000.4	103
3D graphene//Fe_3O_4/graphene	60–90	2587	104
PJ-AC//PrG-based Li-HEC	76–162	4500	105
TiO_2-(reduced graphene oxide)//AC	8.9–42	8000	106
MnNCN//AC	10–103	8533	107
B-Si/SiO_2/C//PSC	89–128	9704	108
CNT-threaded TiO_2//CNT-AC	22.3–59.6	13 900	108
3D-MnO/CNS//3D-CNS-1 : 2	83–184	18 000	110
m-Nb_2O_5-C//AC	15–74	18 510	111
MnO@GNS//HNC	83.25–127	25 000	112
Fe_3O_4@NC//HNC	95–185	28 000	113

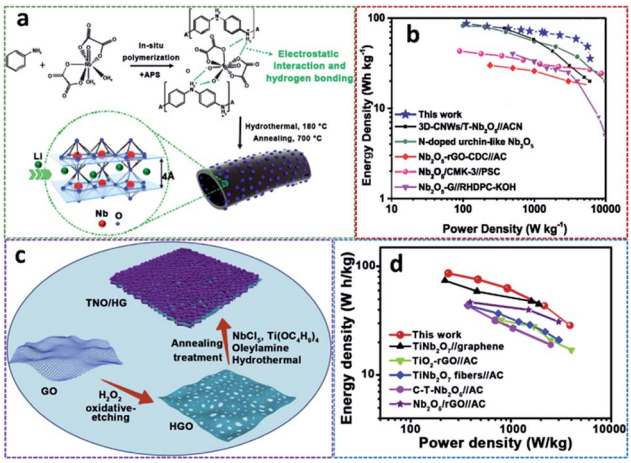

Fig. 7 (a) Schematic of N-NbOC material, (b) Ragone plot of N-NbOC//AC (modified from ref. 116, copyright permission from Elsevier); (c) schematic of the process for fabricating the TNO/HG electrode, (d) Ragone plot of TNO/HG//AC with other LIHSCDs (modified from ref. 118, copyright permission from Elsevier).

sluggish Faradaic anode and the rapid non-Faradaic capacitive cathode. Metal oxide electrode materials also have major applications in NIHSCDs due to the large tunnels in the materials and sensitive dynamics. Lee *et al.*[23] synthesized a nanocomposite comprising Nb_2O_5@carbon core–shell nanoparticles (Nb_2O_5@CNPs) and reduced graphene oxide (rGO), and the NIHSCD using the Nb_2O_5@C/rGO-50 anode and activated carbon (MSP-20) cathode delivered high energy/power densities (76 W h kg^{-1} at 20 800 W kg^{-1}). Fan *et al.*[122] reported highly active $Na_2Ti_3O_7$ nanosheets coated on an activated carbon fiber (Fig. 8a) as a high energy density intercalation-type anode electrode. When fabricated into an NIHSCD with an ionic adsorption cathode based on active carbon fiber (Fig. 8b), the assembled Na-ion hybrid capacitor provided an excellent specific capacitance of 76.8 F g^{-1} at 1 A g^{-1} and a superior energy density of 127.73 W h kg^{-1} at 95.79 W kg^{-1} within a wide operating window of 3.0 V (Fig. 8c).

The cathode materials are also of great concern to enhance the electrochemical performances of NIHSCDs. Chen *et al.*[123] displayed a simple electrochemical route to first synthesize a $NaMnO_2$ cathode for NIHSCDs. The study mainly emphasized the effect of potassium manganese hexacyano ferrate (KMnHCF) on the stability in a Na_2SO_4 electrolyte. The excellent pseudocapacitive behaviour of $Na_{0.21}MnO_2$ in the modified Na_2SO_4 electrolyte was demonstrated with excellent structural stability in the intercalation/de-intercalation of Na^+ during the charge/discharge process. Finally, the assembled NIHSCD exhibited a large operational voltage window (0–2.7 V, Fig. 8d) and a high capacitance retention of 86.7% without any water splitting after 1000 cycles. Extraordinarily, the Na-ion hybrid capacitor could operate a 2.1 V red LED (Fig. 8e).

3.3.3 Other metal-ion hybrid supercapacitor devices. To date, metal oxide materials have been adopted in various ion

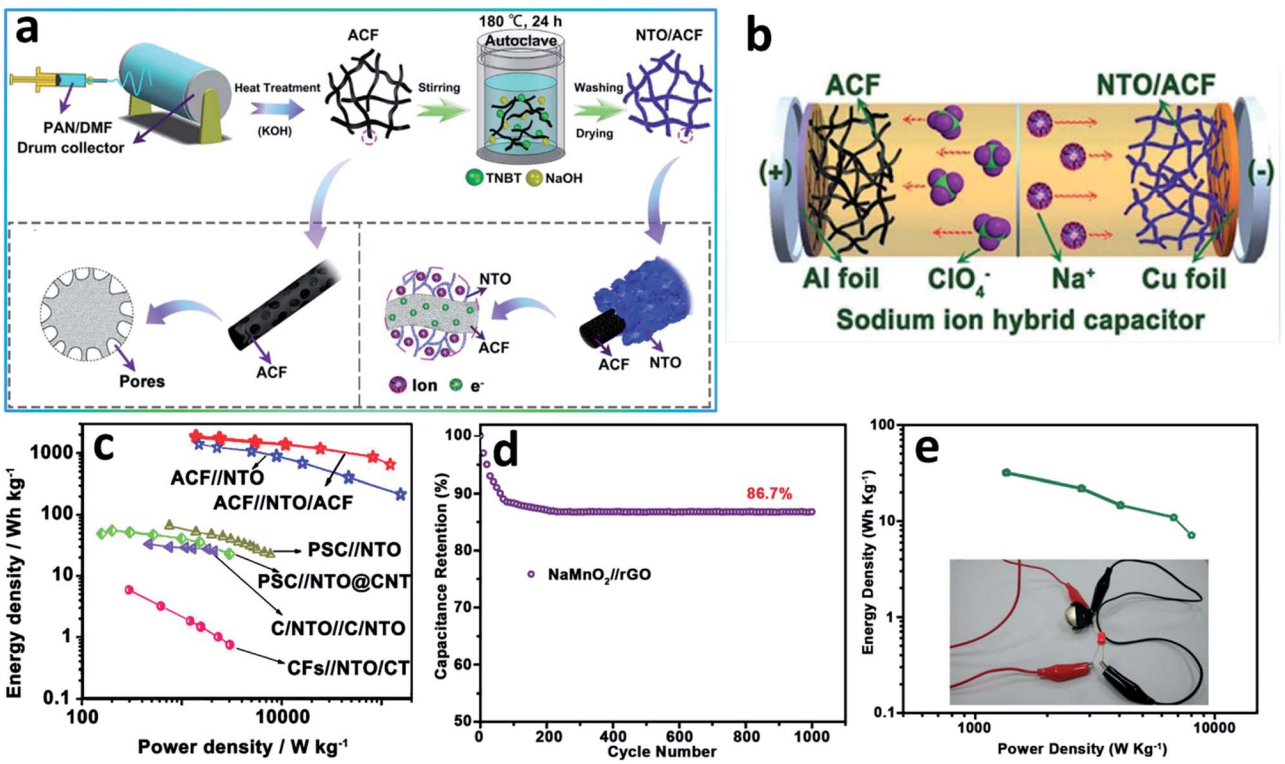

Fig. 8 (a) Schematic of the NTO/ACF nanocomposite, (b) illustration of the fabrication for NIHSCD and (c) Ragone plots compared with other reported works (modified from ref. 122, copyright permission from Wiley-VCH); (d) capacitance retention after 1000 cycles and (e) Ragone plot of the asymmetric $Na_{0.21}MnO_2$//rGO NIHSCD assembled as a CR2032 coin cell (modified from ref. 123, copyright permission from Wiley-VCH).

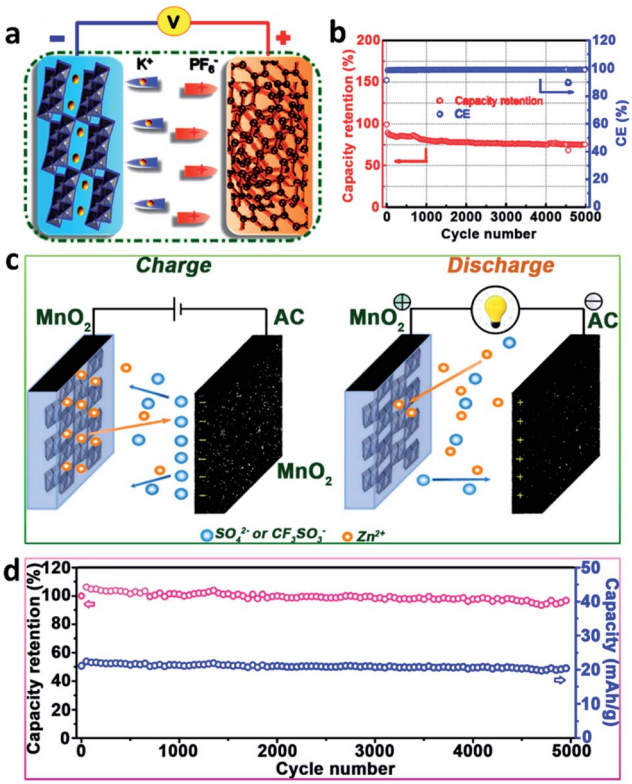

Fig. 9 (a) Schematic and (b) long-term cycling stability at the current density of 1 A g^{-1} of a NGC//KTO KIHSCD (modified from ref. 125, copyright permission from the American Chemical Society); (c) schematic illustration and (d) cycling stability of a designed MnO_2//AC ZIHSCD (modified from ref. 126, copyright permission from Elsevier).

hybrid supercapacitor devices and investigated in large quantities, except for the above Li-ion hybrid and Na-ion hybrid supercapacitor devices. As early as 1999, Goodenough *et al.*[124] had demonstrated the fact that K^+ can work in a Faradaic capacitor as the reactive ions. However, following, there was a long hiatus in the study of potassium ion hybrid supercapacitor devices (KIHSCD). Last year, a $K_2Ti_6O_{13}$ microscaffold anode material of KIHSCD was successfully established by Zhang *et al.*.[125] The hybrid device consisted of a prepared $K_2Ti_6O_{13}$ anode, a cathode of N-doped nanoporous graphenic carbon (NGC) and a non-aqueous potassium-based electrolyte (Fig. 9a). Such a KIHSCD exhibited a battery-like high energy density of 58.2 W h kg^{-1} and supercapacitor-like high power density of 7200 W kg^{-1}. The device achieved an outstanding cycling stability with a capacity retention of 75.5% after 5000 cycles (Fig. 9b).

Considering the advantages of high storage abundance, low flammability and high stability of Zn metal, the Zn-ion hybrid supercapacitor device (ZIHSCD) is becoming one of the optimal choices. Xu *et al.*[126] applied a multivalent ion storage mechanism to construct a high performance aqueous ZIHSCD. Reversible insertion/extraction of Zn^{2+} in a MnO_2 nanorods cathode and ion adsorption/desorption on the surface of the activated carbon anode were established as the energy storage mechanism (Fig. 9c). They further optimized the electrochemical performances by adding Mn^{2+} cations into the $ZnSO_4$ electrolyte to enhance the energy density of the ZIHSCD, while anion replacement of SO_4^{2-} by $CF_3SO_3^-$ effectively inhibited the manganese dissolution and $Zn_4(OH)_6SO_4 \cdot nH_2O$ phase formation. As a result, the as-prepared MnO_2//2 M $ZnSO_4$ (aq)//AC ZIHSCD displayed an excellent capacity of 54.1 mA h g^{-1}, a high energy density of 34.8 W h kg^{-1} and a good cycling stability, with a capacity retention of 93.4% over 5000 cycles (Fig. 9d).

Al-ion hybrid supercapacitor devices (AIHSCDs) have come into existence over the years. The fact that Al is the most abundant metal element in the Earth's crust makes AIHSCD occupy a vantage position, other than Li/Na-ion hybrid supercapacitors. Moreover, an Al^{3+}/Al redox couple contributes three electrons during the electrochemical reaction, which offers viable energy storage capacity.[127]

4. Conclusion and prospectives

In brief, bimetallic oxide materials provide a lot of probabilities to elevate asymmetric supercapacitors to achieve a battery-level energy density, verifying many progress reports in terms of aqueous asymmetric and hybrid supercapacitors. By adjusting the composition and nanostructure of the bimetallic oxides and compositing various carbons appropriately, bimetallic oxides have displayed a continuous improvement in conductivity, surface specific area and the abundance of electrochemically active sites compared to their bulk counterparts, further leading to a tremendous boost in their electrochemical properties. Moreover, novel bimetallic oxides with multiple characteristics as cathodes have exhibited fascinating elasticity and admirable electrochemical properties in a broad working voltage window for designing and fabricating high voltage devices. Particularly, based on the composition and concentration of the electrolytes, a reasonable adjustment of the species and contents of the bimetallic oxides are demanded to balance the relationship among the electric conductivity, porosity, theoretical specific capacity and electrochemically active sites. Specifically, with regard to asymmetric systems, bimetallic oxide/carbon composites with high conductivity and specific capacitance skillfully help reduce mass disparities between the cathode and anode, and therefore enhance the energy density while keeping the power density constant. It also helps to develop hybrid systems by adopting organic electrolytes, and pushes this energy density to a higher level.

Agreement has been reached that novel bimetallic oxide/C composites are conducive to increasing the capacitive properties by making the best use of their advantages of each compound. Nevertheless, the exploration of the physicochemical characteristics and the essential reaction mechanisms involved in hybrid systems are still at the initial stage, in spite of them obtaining excellent electrochemical performances. In addition to conventional preparation methods, low consumption, green, environment-friendly and moderate preparation technologies on account of molecule assemblies are urgently required for the steerable combination of two metal elements, especially by realizing the controllable doping of

metal types and counter-content. Moreover, a point worth emphasizing is that oxygen vacancies generated by various means are well received in bimetallic oxides, which would comparatively enhance the capacitive properties in virtue of the adequate active sites and higher carrier/donor density. Reasonably selecting an appropriate matching of the above methods should be done according to the concrete demands of various supercapacitor systems.

Besides, various metal-ion hybrid supercapacitor devices have shown great improvements to a large extent, which indicates metal-ion hybrid supercapacitor devices might be the key to narrowing the gap between conventional batteries and supercapacitors. However, the progress in metal-ion hybrid supercapacitors is still in the primary stage and the energy storage mechanisms are unclear, and thus need further study to comprehend the interfacial reactions between the electrolyte and electrode. Theoretical calculations and simulations are essential to help disclose the possible electrochemical mechanisms at scale. Simultaneously, *in situ* technologies, such as spectroscopy and microscopy, have been on the development upgrade too and are vital to offer straightforward experimental results. Hence, in near-future studies, synthetic method developments and electrochemical mechanisms as well as device configurations demand joint efforts to advance bimetallic oxide-based supercapacitor systems. After persistent efforts, we are fully convinced that the profound understanding will be explored and other kinds of supercapacitor systems (for example, highly flexible and wearable devices) will spring up in the near future.

Conflicts of interest

There are no conflicts to declare.

Acknowledgements

This work was supported by the NSFC (51871123, 51701127, 51571124), Natural Science Foundation of Tianjin (17JCYBJC17900, 18JCYBJC90200), Ministry of Science and Technology (2016-YFA0202500), Ministry of Education (IRT13R30), and 111 Project (B12015).

References

1 G. Wang, L. Zhang and J. Zhang, *Chem. Soc. Rev.*, 2012, **41**, 797–828.
2 G. Yu, L. Hu, N. Liu, H. Wang, M. Vosguerichian, Y. Yang, Y. Cui and Z. Bao, *Nano Lett.*, 2011, **11**, 4438–4442.
3 Q. Lu, J. Chen and J. Xiao, *Angew. Chem., Int. Ed.*, 2013, **52**, 1882–1889.
4 Z. Yu, L. Tetard, L. Zhai and J. Thomas, *Energy Environ. Sci.*, 2015, **8**, 702–730.
5 X. Lu, C. Wang, F. Favier and N. Pinna, *Adv. Energy Mater.*, 2017, **7**, 1601301.
6 Y. Xu, X. Wang, C. An, Y. Wang, L. Jiao and H. Yuan, *J. Mater. Chem. A*, 2014, **2**, 16480–16488.
7 H. Gao, Y. Li, H. Zhao, J. Xiang and Y. Cao, *Electrochim. Acta*, 2018, **262**, 241–251.
8 S. Raj, P. Kar and P. Roy, *Chem. Commun.*, 2018, **54**, 12400–12403.
9 C. An, Y. Wang, Y. Huang, Y. Xu, L. Jiao and H. Yuan, *Nano Energy*, 2014, **10**, 125–134.
10 L. Huang, D. Chen, Y. Ding, S. Feng, Z. Wang and M. Liu, *Nano Lett.*, 2013, **13**, 3135–3139.
11 S. Chen, M. Xue, Y. Pan, L. Zhu and S. Qiu, *J. Mater. Chem. A*, 2015, **3**, 20145–20152.
12 F. Wang, X. Wu, X. Yuan, Z. Liu, Y. Zhang, L. Fu, Y. Zhu, Q. Zhou, Y. Wu and W. Huang, *Chem. Soc. Rev.*, 2017, **46**, 6816–6854.
13 R. Salunkhe, Y. Kaneti and Y. Yamauchi, *ACS Nano*, 2017, **11**, 5293–5308.
14 L. Zhang, D. Shi, T. Liu, M. Jaroniec and J. Yu, *Mater. Today*, 2019, **25**, 35–65.
15 Y. Dong, Y. Wang, Y. Xu, C. Chen, Y. Wang, L. Jiao and H. Yuan, *Electrochim. Acta*, 2017, **225**, 39–46.
16 X. Xiao, G. X. Zhang, Y. X. Xu, H. L. Zhang, X. T. Guo, Y. Liu and H. Pang, *J. Mater. Chem. A*, 2019, **7**, 17266.
17 X. T. Guo, Y. Z. Zhang, F. Zhang, Q. Li, D. H. Anjum, H. F. Liang, Y. Liu, C. Liu, H. N. Alshareef and H. Pang, *J. Mater. Chem. A*, 2019, **7**, 15969.
18 J. Y. Ma, X. T. Guo, Y. Yan, H. G. Xue and H. Pang, *Adv. Sci.*, 2018, **5**, 1700986.
19 X. R. Li, J. L. Wei, Q. Li, S. S. Zhang, Y. X. Xu, P. Du, C. Y. Chen, J. Y. Zhao, H. G. Xue, Q. Xu and H. Pang, *Adv. Funct. Mater.*, 2019, **28**, 1800886.
20 H. Kim, J. Cook, H. Lin, J. Ko, S. Tolbert, V. Ozolins and B. Dunn, *Nat. Mater.*, 2016, **16**, 454.
21 M. Javed, N. Shaheen, S. Hussain, J. Li, S. Shah, Y. Abbas, M. Ahmad, R. Raza and W. Mai, *J. Mater. Chem. A*, 2019, **7**, 946–957.
22 J. Ding, W. Hu, E. Paek and D. Mitlin, *Chem. Rev.*, 2018, **118**, 6457–6498.
23 E. Lim, C. Jo, M. Kim, M. Kim, J. Chun, H. Kim, J. Park, K. Roh, K. Kang, S. Yoon and J. Lee, *Adv. Funct. Mater.*, 2016, **26**, 3711–3719.
24 S. Hussain and J. Yu, *Chem. Eng. J.*, 2019, **361**, 1030–1042.
25 X. He, R. Li, J. Liu, Q. Liu, R. Chen, D. Song and J. Wang, *Chem. Eng. J.*, 2018, **334**, 1573–1583.
26 S. Zhang, B. Yin, C. Liu, Z. Wang and D. Gu, *Chem. Eng. J.*, 2017, **312**, 296–305.
27 J. Wang, W. Dou, X. Zhang, W. Han, X. Mu, Y. Zhang, X. Zhao, Y. Chen, Z. Yang, Q. Su, E. Xie, W. Lan and X. Wang, *Electrochim. Acta*, 2017, **224**, 260–268.
28 H. Pang, X. Li, Q. Zhao, H. Xue, W.-Y. Lai, Z. Hu and W. Huang, *Nano Energy*, 2017, **35**, 138–145.
29 Q. Meng, K. Cai, Y. Chen and L. Chen, *Nano Energy*, 2017, **36**, 268–285.
30 C. Zhang, C. L. Lei, C. Cen, S. L. Tang, M. S. Deng, Y. L. Li and Y. W. Du, *Electrochim. Acta*, 2018, **260**, 814–822.
31 J. S. Xu, Y. D. Sun, M. J. Lu, L. Wang, J. Zhang, J. H. Qian and X. Y. Liu, *Chem. Eng. J.*, 2018, **334**, 1466–1476.
32 K. B. Xu, J. M. Yang and J. Q. Hu, *J. Colloid Interface Sci.*, 2018, **511**, 456–462.

33 B. Guan, A. Kushima, L. Yu, S. Li, J. Li and X. Lou, *Adv. Mater.*, 2017, **29**, 1605902.
34 C. Guan, W. Zhao, Y. Hu, Z. Lai, X. Li, S. Sun, H. Zhang, A. Cheetham and J. Wang, *Nanoscale Horiz.*, 2017, **2**, 99–105.
35 X. Zhang, A. Chen, M. Zhong, Z. Zhang, X. Zhang, Z. Zhou and X. Bu, *Electrochem. Energy Rev.*, 2019, **2**, 29–104.
36 G. Zhong, D. Liu and J. Zhang, *J. Mater. Chem. A*, 2018, **6**, 1887–1899.
37 S. Lu, M. Jin, Y. Zhang, Y. Niu, J. Gao and C. M. Li, *Adv. Energy Mater.*, 2018, **8**, 1702545.
38 R. Zou, H. Quan, M. Pan, S. Zhou, D. Chen and X. Luo, *Electrochim. Acta*, 2018, **292**, 31–38.
39 J. Lin, H. Jia, H. Liang, S. Chen, Y. Cai, J. Qi, C. Qu, J. Cao, W. Fei and J. Feng, *Adv. Sci.*, 2018, **5**, 1700687.
40 W. Lu, S. Huang, L. Miao, M. Liu, D. Zhu, L. Li, H. Duan, Z. Xu and L. Gan, *Chinese Chem. Lett.*, 2017, **28**, 1324–1329.
41 Y. Zhang and S. J. Park, *Carbon*, 2017, **122**, 287–297.
42 Z. J. Shi, L. Xing, Y. Liu, Y. F. Gao and J. R. Liu, *Carbon*, 2018, **129**, 819–825.
43 H. Kashani, L. Y. Chen, Y. Ito, J. H. Han, A. Hirata and M. W. Chen, *Nano Energy*, 2016, **19**, 391–400.
44 C. S. Huang, Y. J. Li, N. Wang, Y. R. Xue, Z. C. Zuo, H. B. Liu and Y. L. Li, *Chem. Rev.*, 2018, **118**, 7744–7803.
45 H. Shang, Z. C. Zuo, L. Li, F. Wang, H. B. Liu, Y. J. Li and Y. L. Li, *Angew. Chem., Int. Ed.*, 2018, **57**, 774–778.
46 X. Y. He, Y. H. Zhao, R. R. Chen, H. S. Zhang, J. Y. Liu, Q. Liu, D. L. Song, R. M. Li and J. Wang, *ACS Sustainable Chem. Eng.*, 2018, **6**, 14945–14954.
47 T. Ling, P. Da, X. Zheng, B. Ge, Z. Hu, M. Wu, X. Du, W. Hu, M. Jaroniec and S. Qiao, *Sci. Adv.*, 2018, **4**, 6261.
48 G. Li, M. Chen, Y. Ouyang, D. Yao, L. Lu, L. Wang, X. Xia, W. Lei, S. Chen, D. Mandler and Q. Hao, *Appl. Surf. Sci.*, 2019, **469**, 941–950.
49 S. Yang, Y. Liu, Y. Hao, X. Yang, W. Iii, X. L. Zhang and B. Cao, *Adv. Sci.*, 2018, **5**, 1700659.
50 S. Liu, Y. Yin, D. Ni, K. S. Hui, M. Ma, S. Park, K. N. Hui, C. Ouyang and S. C. Jun, *Energy Storage Mater.*, 2019, **22**, 384–396.
51 F. Wang, X. Wu, X. Yuan, Z. Liu, Y. Zhang, L. Fu, Y. Zhu, Q. Zhou, Y. Wu and W. Huang, *Chem. Soc. Rev.*, 2017, **46**, 6816–6854.
52 L. Suo, O. Borodin, T. Gao, M. Olguin, J. Ho, X. Fan, C. Luo, C. Wang and K. Xu, *Science*, 2015, **350**, 9367.
53 M. Zhang, Y. Li and Z. Shen, *J. Power Sources*, 2019, **414**, 479–485.
54 M. Yu, Y. Lu, H. Zheng and X. Lu, *Chem.–Eur. J.*, 2018, **24**, 3639–3649.
55 Lithium Bid(pentafluoroethanesulfonyl)imide, TCI America, #L0267.
56 M. R. Lukatskaya, J. I. Feldblyum, D. G. Mackanic, F. Lissel, D. L. Michels, Y. Cui and Z. N. Bao, *Energy Environ. Sci.*, 2018, **11**, 2876–2883.
57 L. M. Suo, O. Borodin, W. Sun, X. L. Fan, C. Y. Yang, F. Wang, T. Gao, Z. H. Ma, M. Schroeder, A. Cresce, S. M. Russell, M. Armand, A. Angell, K. Xu and C. S. Wang, *Angew. Chem.*, 2016, **128**, 7252–7257.
58 Q. Y. Dou, S. L. Lei, D. W. Wang, Q. N. Zhang, D. W. Xiao, H. W. Guo, A. P. Wang, H. Yang, Y. L. Li, S. Q. Shi and X. B. Yan, *Energy Environ. Sci.*, 2018, **11**, 3212–3219.
59 Z. Pan, J. Yang, Q. Zhang, M. Liu, Y. Hu, Z. Kou, N. Liu, X. Yang, X. Ding, H. Chen, J. Li, K. Zhang, Y. Qiu, Q. Li, J. Wang and Y. Zhang, *Adv. Energy Mater.*, 2019, **9**, 1802753.
60 Y. Shao, M. El-Kady, J. Sun, Y. Li, Q. Zhang, M. Zhu, H. Wang, B. Dunn and R. B. Kaner, *Chem. Rev.*, 2018, **118**, 9233–9280.
61 N. Choudhary, C. Li, J. Moore, N. Nagaiah, L. Zhai, Y. Jung and J. Thomas, *Adv. Mater.*, 2017, **29**, 1605336.
62 X. Lu, C. Wang, F. Favier and N. Pinna, *Adv. Energy Mater.*, 2017, **7**, 1601301.
63 S. Sheng, W. Liu, K. Zhu, K. Cheng, K. Ye, G. Wang, D. Cao and J. Yan, *J. Colloid Interface Sci.*, 2019, **536**, 235–244.
64 J. Zhao, Z. Li, X. Yuan, Z. Yang, M. Zhang and A. Meng, *Adv. Energy Mater.*, 2018, **8**, 1702787.
65 R. Sahoo, D. T. Pham, T. H. Lee, T. H. T. Luu, J. Seok and Y. H. Lee, *ACS Nano*, 2018, **12**, 8494–8505.
66 S. Trasattl and G. Buzzanca, *J. Electroanal. Chem.*, 1971, **29**, l–5.
67 S. Kong, K. Cheng, T. Ouyang, Y. Gao, K. Ye, G. Wang and D. Cao, *Electrochim. Acta*, 2017, **246**, 433–442.
68 S. Zhu, L. Li, J. Liu, H. Wang, T. Wang, Y. Zhang, L. Zhang, R. S. Ruoff and F. Dong, *ACS Nano*, 2018, **12**, 1033–1042.
69 T. Xiong, T. L. Tan, L. Lu, W. S. V. Lee and J. Xue, *Adv. Energy Mater.*, 2018, **8**, 1702630.
70 Y. Liu, L. Guo, X. Teng, J. Wang, T. Hao, X. He and Z. Chen, *Electrochim. Acta*, 2019, **300**, 9–17.
71 N. Jabeen, A. Hussain, Q. Xia, S. Sun, J. Zhu and H. Xia, *Adv. Mater.*, 2017, **29**, 1700804.
72 T. Liu, L. Zhang, W. You and J. Yu, *Small*, 2018, **14**, 1702407.
73 G. Saeed, S. Kumar, N. H. Kim and J. H. Lee, *Chem. Eng. J.*, 2018, **352**, 268–276.
74 F. Zheng, C. Xi, J. Xu, Y. Yu, W. Yang, P. Hu, Y. Li, Q. Zhen, S. Bashir and J. L. Liu, *J. Alloys Compd.*, 2019, **772**, 933–942.
75 X. Yuan, B. Chen, X. Wu, J. Mo, Z. Liu, Z. Hu, z. Liu, c. Zhou, h. Yang and y. Wu, *Chin. J. Chem.*, 2017, **35**, 61–66.
76 W. Zhang, H. Lin, H. Kong, H. Lu, Z. Yang and T. Liu, *Int. J. Hydrogen Energy*, 2014, **39**, 17153–17161.
77 X. Hong, S. Li, R. Wang and J. Fu, *J. Alloys Compd.*, 2019, **775**, 15–21.
78 S. D. Jagadale, A. M. Teli, S. V. Kalake, A. D. Sawant, A. D. Sawant and A. A. Yadav, *J. Electroanal. Chem.*, 2018, **816**, 99–106.
79 S. Wang, J. Hu, L. Liang, X. Li, J. Cao, Q. Wang, A. Wang, X. Li, L. Qu and Y. Lu, *Electrochim. Acta*, 2019, **293**, 273–282.
80 X. Ren, C. Guo, L. Xu, T. Li, L. Hou and Y. Wei, *ACS Appl. Mater. Interfaces*, 2015, **7**, 19930–19940.
81 S. E. Moosavifard, M. F. El-Kady, M. S. Rahmanifar, R. B. Kaner and M. F. Mousavi, *ACS Appl. Mater. Interfaces*, 2015, **7**, 4851–4860.
82 Y. Xue, T. Chen, S. Song, P. Kim and J. Bae, *Nano Energy*, 2019, **56**, 751–758.
83 M. M. Vadiyar, S. S. Kolekar, J. Chang, Z. Ye and A. V. Ghule, *ACS Appl. Mater. Interfaces*, 2017, **9**, 26016–26028.

84 J. Zhao, Z. J. Li, X. C. Yuan, Z. Yang, M. Zhang, A. Meng and Q. D. Li, *Adv. Energy Mater.*, 2018, **8**, 1702787.
85 X. Chang, L. Zang, S. Liu, M. Wang, H. Guo, C. Wang and Y. Wang, *J. Mater. Chem. A*, 2018, **6**, 9190.
86 V. S. Kumbhar and D. H. Kim, *Electrochim. Acta*, 2018, **271**, 284–296.
87 C. Chen, S. Wang, X. Luo, W. J. Gao, G. J. Huang, Y. Zeng and Z. H. Zhu, *J. Power Sources*, 2019, **409**, 112–122.
88 S. C. Sekhar, G. Nagaraju and J. S. Yu, *Nano Energy*, 2018, **48**, 81–92.
89 T. Lv, M. X. Liu, D. Zhu, L. Gan and T. Chen, *Adv. Mater.*, 2018, **30**, 1705489.
90 X. Lu, M. Yu, G. Wang, Y. Tong and Y. Li, *Energy Environ. Sci.*, 2014, **7**, 2016.
91 D. P. Dubal, N. R. Chodankar, D. H. Kim and P. Gomez-Romero, *Chem. Soc. Rev.*, 2018, **47**, 2065–2129.
92 C. Chen, J. Cao, Q. Lu, X. Wang, L. Song, Z. Niu and J. Chen, *Adv. Funct. Mater.*, 2017, **27**, 1604639.
93 Z. Zhang, K. Chi, F. Xiao and S. Wang, *J. Mater. Chem. A*, 2015, **3**, 12828.
94 Z. Zhang, F. Xiao, Y. Guo, S. Wang and Y. Liu, *ACS Appl. Mater. Interfaces*, 2013, **5**, 2227.
95 Z. Zhang, F. Xiao, J. Xiao and S. Wang, *J. Mater. Chem. A*, 2015, **3**, 11817.
96 Z. Zhang, F. Xiao and S. Wang, *J. Mater. Chem. A*, 2015, **3**, 11215.
97 Q. Wang, L. Shao, Z. Ma, J. Xu and C. Wang, *Electrochim. Acta*, 2018, **281**, 2582.
98 T. G. Yun, M. Park, D. H. Kim, D. Kim, J. Y. Chong, J. G. Bae, S. M. Han and I. D. Kim, *ACS Nano*, 2019, **13**, 3141.
99 Z. Zhang, F. Xiao, L. Qian, J. Xiao, S. Wang and Y. Liu, *Adv. Energy Mater.*, 2014, **4**, 1400064.
100 H. Wang, C. Zhu, D. Chao, Q. Yan and H. Fan, *Adv. Mater.*, 2017, **29**, 201604639.
101 W. Zuo, R. Li, C. Zhou, Y. Li, J. Xia and J. Liu, *Adv. Sci.*, 2017, **4**, 1600539.
102 Z. Chen, V. Augustyn, X. L. Jia, Q. F. Xiao, B. Dunn and Y. F. Lu, *ACS Nano*, 2012, **6**, 4319–4327.
103 H. P. Du, H. Yang, C. S. Huang, J. J. He, H. B. Liu and Y. L. Li, *Nano Energy*, 2016, **22**, 615–622.
104 F. Zhang, T. F. Zhang, X. Yang, L. Zhang, K. Leng, Y. Huang and Y. S. Chen, *Energy Environ. Sci.*, 2013, **6**, 1623–1632.
105 P. Sennu, V. Aravindan, M. Ganesan, Y. G. Lee and Y. S. Lee, *ChemSusChem*, 2016, **9**, 849–854.
106 H. Kim, M. Y. Cho, M. H. Kim, K. Y. Park, H. Gwon, Y. S. Lee, K. C. Roh and K. Kang, *Adv. Energy Mater.*, 2013, **3**, 1500–1506.
107 C. F. Liu, C. K. Zhang, H. Y. Fu, X. H. Nan and G. Z. Cao, *Adv. Energy Mater.*, 2017, **7**, 1601127.
108 R. Yi, S. Chen, J. X. Song, M. L. Gordin, A. Manivannan and D. H. Wang, *Adv. Funct. Mater.*, 2014, **24**, 7433–7439.
109 Z. Chen, Y. Yuan, H. H. Zhou, X. L. Wang, Z. H. Gan, F. S. Wang and Y. F. Lu, *Adv. Mater.*, 2014, **26**, 339–345.
110 H. L. Wang, Z. W. Xu, Z. Li, K. Cui, J. Ding, A. Kohandehghan, X. H. Tan, B. Zahiri, B. C. Olsen, C. M. B. Holt and D. Mitlin, *Nano Lett.*, 2014, **14**, 1987–1994.
111 E. Lim, H. Kim, C. S. Jo, J. Y. Chun, K. Ku, S. Kim, H. I. Lee, I. S. Nam, S. H. Yoon, K. Kang and J. Lee, *ACS Nano*, 2014, **8**, 8968–8978.
112 M. Yang, Y. R. Zhong, J. J. Ren, X. L. Zhou, J. P. Wei and Z. Zhou, *Adv. Energy Mater.*, 2015, **5**, 1500550.
113 C. H. An, X. Z. Liu, Z. Gao and Y. Ding, *Sci. China Mater.*, 2017, **60**, 217–227.
114 Y. Ouyang, H. Ye, X. Xia, X. Jiao, G. Li, S. Mutahir, L. Wang, D. Mandler, W. Lei and Q. Hao, *J. Mater. Chem. A*, 2019, **7**, 3228–3237.
115 L. Chen, W. Zhai, L. Chen, D. Li, X. Ma, Q. Ai, X. Xu, G. Hou, L. Zhang, J. Feng, P. Si and L. Ci, *J. Power Sources*, 2018, **392**, 116–122.
116 S. Hemmati, G. Li, X. Wang, Y. Ding, Y. Pei, A. Yu and Z. Chen, *Nano Energy*, 2019, **56**, 118–126.
117 W. Qu, F. Han, A. Lu, C. Xing, M. Qiao and W. Li, *J. Mater. Chem. A*, 2014, **2**, 6549.
118 X. Jiao, Q. Hao, X. Xia, D. Yao, Y. Ouyang and W. Lei, *J. Power Sources*, 2018, **403**, 66–75.
119 V. Aravindan, M. Ulaganathan and S. Madhavi, *J. Mater. Chem. A*, 2016, **4**, 7538–7548.
120 E. Lim, C. Jo, M. S. Kim, M. Kim, J. Chun, H. Kim, J. Park, K. C. Roh, K. Kang, S. Yoon and J. Lee, *Adv. Funct. Mater.*, 2016, **26**, 3711–3719.
121 X. Wang, Q. Li, L. Zhang, Z. Hu, L. Yu, T. Jiang, C. Lu, C. Yan, J. Sun and Z. Liu, *Adv. Mater.*, 2018, **30**, 1800963.
122 X. Qiu, X. Zhang and L. Fan, *J. Mater. Chem. A*, 2018, **6**, 16186.
123 N. Karikalan, C. Karuppiah, S. Chen, M. Velmurugan and P. Gnanaprakasam, *Chem.–Eur. J.*, 2017, **23**, 2379–2386.
124 H. Lee and J. B. Goodenough, *J. Solid State Chem.*, 1999, **148**, 81–84.
125 S. Dong, Z. Li, Z. Xing, X. Wu, X. Ji and X. Zhang, *ACS Appl. Mater. Interfaces*, 2018, **10**, 15542–15547.
126 X. Ma, J. Cheng, L. Dong, W. Liu, J. Mou, L. Zhao, J. Wang, D. Ren, J. Wu, C. Xu and F. Kang, *Energy Storage Mater.*, 2019, **20**, 335–342.
127 F. Wang, Z. Liu, X. Wang, X. Yuan, X. Wu, Y. Zhu, L. Fu and Y. Wu, *J. Mater. Chem. A*, 2016, **4**, 5115–5123.

